Seismic wavefield simulation using Finite Element Method in a visco-Poroleastic medium

Sudhanshu Pandey[a], Pritam Chakraborty[a], Dibakar Ghosal[a], Rahul Singh[b]*
[a]*Indian Institute of Technology Kanpur,* [b]*Oil and Natural Gas Corporation Ltd*

pandeysd@iitk.ac.in

Keywords

Biot's equations, Finite Element Method, Shot gather.

Summary

The complex rheology of geophysical media is suitably represented by the Biot's model that accurately captures wave propagation in fluid saturated, porous solid. In hydrocarbon and gas hydrate reservoir exploration activities, the use of this model can be instrumental in quantifying reservoir properties from the acquired shot gathers. However, parameter exploration and inverse modeling may be required, thus necessitating numerous simulations of initio-boundary value problems, involving Biot's equation. Thus, a Finite Element Method (FEM) based tool is developed in this work that can be used to solve the Biot's model for realistic geophysical problems and characterize the physical properties of the hydrocarbon reservoirs inverting seismic datasets.

Introduction

Full wavefield inversion method can assist in identifying hydrocarbon and gas hydrate reservoirs inverting shot gathers. The method relies on suitable models that can accurately represent the dynamics of the reservoir. The models, typically initio-boundary value equations, are solved using some numerical scheme. The synthetic waveforms thus obtained from the simulations are compared with the observed shot gather and the differences are minimized iteratively to predict the physical properties of the subsurface. Thus, the predictability of the full wavefield inversion method relies strongly on the accuracy of the model and the numerical scheme being utilized.

The complex rheology of shallow subsurface can be reasonably assumed as a porous solid with saturated fluid. Models proposed by Biot (Biot, 1956a; Biot, 1956b) and Hickey (Hickey et al., 1997) consider poro-elasto-dynamics with attenuation for fluid filled porous solid, and, are widely used in modeling subsurface realistically. While Hickey's model further considers thermo-mechanical coupling and porosity perturbations due to local pressure variations, it provides similar waveforms as of Biot's equations (Quiroga-Goode et al., 2005). Thus, the present work uses the Biot's law to represent fluid saturated porous media.

Different methods have been used in the seismology community to solve elasto and poro-elasto-dynamical behavior of subsurface (Carcione et al., 2002). The methods can be classified under direct, integral and asymptotic expansion based schemes. In the direct method, finite difference or finite element based numerical techniques are utilized to obtain the synthetic shot gather. The direct method has no assumption of superposition and frequency truncation made in the integral and asymptotic expansion based schemes, respectively. Thus, the direct method is more accurate than the other two and thus chosen in this work. Furthermore, the Finite Element Method (FEM) has been chosen under direct techniques since the integral representation of the differential form improves the accuracy of the numerical results and the flexibility to use irregular grid allows handling arbitrary geology (Carcione et al., 2002).

Poro-Visco-Elasto-Dynamics Model

The Biot's poro-elasto-dynamics model with linear attenuation as presented in Martin et al., 2008, is utilized in this work. In the model, the inertias of the solid and saturated fluid media in the pores are considered following

$$(1-\phi)\rho_s \frac{\partial^2 u_i^s}{\partial t^2} + \phi\rho_f \frac{\partial^2 u_i^f}{\partial t^2} = \frac{\partial \sigma_{ij}}{\partial x_j} \qquad (1)$$

$$(1-a)\rho_f \frac{\partial^2 u_i^s}{\partial t^2} + a\rho_f \frac{\partial^2 u_i^f}{\partial t^2} = -\frac{\partial p^f}{\partial x_i} - K\phi \frac{\partial u_i^f}{\partial t} + K\phi \frac{\partial u_i^s}{\partial t} \tag{2}$$

where u_i^s, u_i^f, ρ_s, ρ_f, ϕ, p^f, σ_{ij}, K and a are the solid and fluid displacement components, solid and fluid densities, volume fraction of fluid, fluid pressure, effective stress tensor components, viscosity and tortuosity, respectively.

The effective stress tensor of the porous solid is described as a superposition of stress in the solid media and pressure in the saturated pore(s) with fluid as

$$\sigma_{ij} = \sigma_{ij}{}^{s} - \alpha p^f \delta_{ij} \tag{3}$$

where

$$\sigma_{ij}{}^{s} = \left(\lambda \delta_{ij}\delta_{kl} + 2\mu \delta_{ik}\delta_{jl}\right)\varepsilon_{kl}^{s} \tag{4}$$

$$p^f = [\phi - \alpha] M \frac{\partial u_i^s}{\partial x_i} - M\phi \frac{\partial u_i^f}{\partial x_i} \tag{5}$$

In Equations 4 and 5, λ and μ are the Lame's constant of the solid media and M is the bulk modulus of the fluid.

Finite Element Method Representation

The attenuation of the wavefield can be attributed to viscous behavior of the saturated fluid in the pores. While in majority of the models the viscous laws adopted is linear, in order to simplify the problem and obtain an approximate solution, it is not a necessary condition. Thus, in this work it is considered that the attenuation behavior can be non-linear and hence a non-linear FEM solver is developed.

A Galerkin approach is followed to obtain the semi-discrete elemental weak form. The temporal discretization is performed using the Newmark-beta method and the parameters are chosen corresponding to an implicit scheme (Belytschko et al.). The presence of fluid saturated pores in solid can result in a numerically stiff system. The implicit scheme is chosen to provide unconditional stability such that reasonably large time steps can be used.

The discretized system is then linearized and solved using the Newton-Raphson (NR) update algorithm. From the NR method the displacement increments of the solid and fluid media are obtained as

$$\begin{Bmatrix} \Delta u_s \\ \Delta u_f \end{Bmatrix} = -[K]_{Global}^{-1}\{R\}_{Global} \tag{6}$$

where $\{R\}_{Global}$ and $[K]_{Global}$ are the assembled residual vector and stiffness matrix, respectively. These are obtained from the elemental residual vector

$$\{R\}^e = \begin{Bmatrix} R_1 \\ R_2 \end{Bmatrix}^e$$

where

$$\{R_1\}^e = \sum_{ig=1}^{N_g}\left([M_s]\{\ddot{u}_s^{\beta}\} + [M_f]\{\ddot{u}_f^{\beta}\}\right) + \sum_{ig=1}^{N_g}\left([B]^T\{\sigma_s\} - [C]^T \alpha p^f\right)\det(J) w_{ig} \tag{7}$$

and

$$\{R_2\}^e = \sum_{ig=1}^{N_g}\left([M_1]\{\ddot{u}_s^{\beta}\} + [M_2]\{\ddot{u}_f^{\beta}\} - [M_3]\{\dot{u}_s^{\beta}\} + [M_3]\{\dot{u}_f^{\beta}\}\right) - \sum_{ig=1}^{N_g}\left([C]^T \alpha p^f\right)\det(J) w_{ig} \tag{8}$$

and stiffness matrix

$$[K]^e = \begin{bmatrix} K_{11} & K_{12} \\ K_{21} & K_{22} \end{bmatrix}^e$$

where

$$[K_{11}]^e = \sum_{ig=1}^{N_g}[M_s] + \sum_{ig=1}^{N_g}[B]^T[\partial\sigma/\partial\varepsilon][B]\det(J) w_{ig} \tag{9}$$

$$[K_{12}]^e = \sum_{ig=1}^{N_g}[M_f] - \sum_{ig=1}^{N_g}\alpha[C]^T\left[\partial p^f/\partial \varepsilon_V{}^f\right][C]\det(J) w_{ig} \tag{10}$$

$$[K_{21}]^e = \sum_{ig=1}^{N_g}([M_1] - [M_3]) \tag{11}$$

$$[K_{22}]^e = \sum_{ig=1}^{N_g}([M_2] + [M_3]) - \sum_{ig=1}^{N_g}\alpha[C]^T\left[\partial p^f/\partial \varepsilon_V{}^f\right][C]\det(J) w_{ig} \tag{12}$$

In the above equations

$$[B] = \begin{bmatrix} 1 & 0 & 0 & 0 \\ 0 & 0 & 0 & 1 \\ 0 & 1 & 1 & 0 \end{bmatrix}[N_x] \tag{13}$$

and

$$[C] = [1 \quad 0 \quad 0 \quad 1][N_x] \tag{14}$$

for two-dimensional problems. $[N_x]$ is the spatial derivative of the shape functions (Belytschko et al.). The example problem shown here is based on bilinear isoparametric shape functions.

Results and Discussions

The workability of the FEM code is verified by analyzing the response of a three layered confined structure. The dimensions of the layers are chosen as 1 m (length) × 0.35 m (height). The FE mesh of the three layered structure is shown in Figure 1.

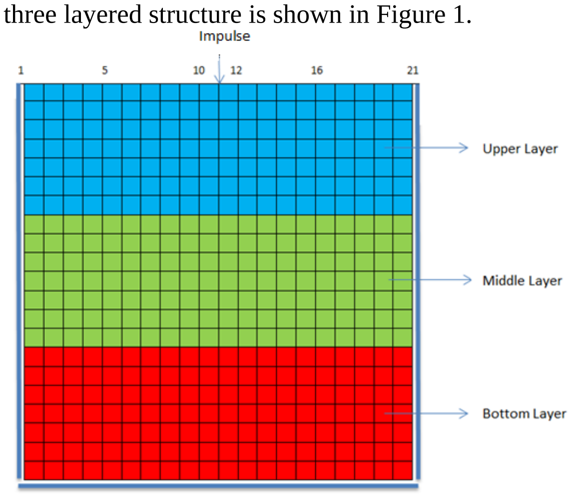

Figure 1: The FE mesh of the 3 layered structure.

Both the layers are considered to fluid saturated porous solid having different elastic properties of the solid media, porosity and tortuosity. The properties utilized for all three layers are shown in Table 1. A single shot is applied at the middle of the top layer as shown in Figure 1. The shot is approximated as a linearly increasing force for a certain time and is shown in Figure 2.

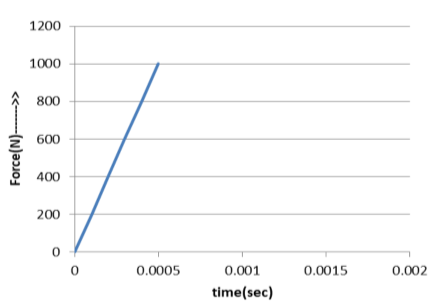

Figure 2: Impulse applied at the centre of the topmost layer.

S.No	Physical Variable	Unit(SI)	Upper Layer	Mid Layer	Bottom Layer
1	Solid Density ρ_s	kg/m^3	2250	2420	2588
2	Fluid Density ρ_f	kg/m^3	1040	998	952.4
3	Porosity ϕ	-	0.01	0.1	0.25
4	Alpha α	-	0.89	0.6	0.3
5	Matrix tortuosity a	-	2.49	2.49	2.49
6	Bulk Modulus M	Pa	7.7×10^9	7.79×10^9	7.79×10^9
7	Damping Viscous Term K	Ns/m^4	3.38×10^5	3.38×10^5	3.38×10^5
8	Shear Modulus μ	m/s	5.2×10^9	10^9	10^8
9	Lame Coefficient λ	Pa	6.7×10^9	10^9	10^8

Table 1. Physical properties of the heterogeneous three-layer model under study

As the shot is applied, the wave front starts to advance from the center of the top layer as shown in Figure 3(a). The front advances radially (Figure 3(b)) and hits the interface, after which the wave spreads length-wise in the middle layer (Figure 3(c)). Subsequently, it hits the second interface and enters the bottom layer (Figure 3(d)) and propagates (Figure 3(e)), to finally hit and get reflected from the bottom face (Figure 3(f)). Comparing Figures 3(e) and (f), it can be argued that the wave gets reflected from the bottom face based on the maximum displacement magnitude contour that significantly reduces in Figures 3(f). The simulation is not carried out further since the confinement starts to cause interaction and the next peak in the shot gather data is not observable.

The single shot gather from this example is shown in Figure 4 and corresponds to the length-wise travel of the wave. The trend corroborates with experimental observations thus illustrating the workability of the code.

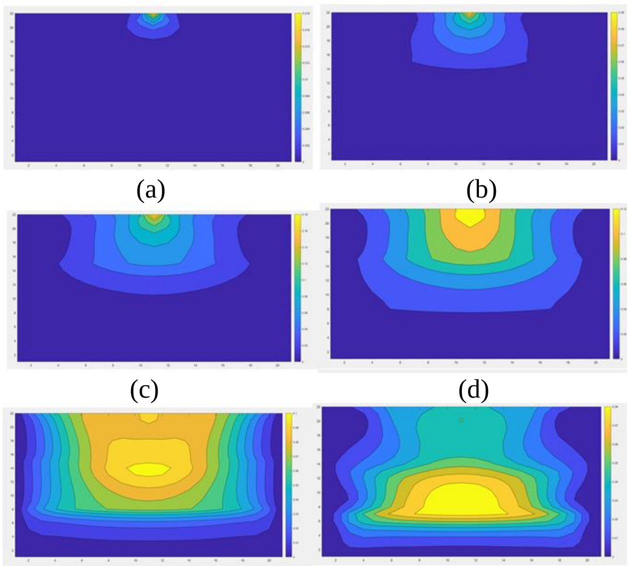

(a) (b) (c) (d) (e) (f)

Figure 3: Contour profile of the magnitude of displacement at different times: (a) t=0.0001 sec, (b) t= 0.0003 sec, the wave hits first interface (c) t=0.0005 sec, (d) t=0.0006 sec, the wave just hits the second interface (e) t=0.0009 sec, just before hitting the side walls (f) t=0.0011 sec, after hitting all the boundaries.

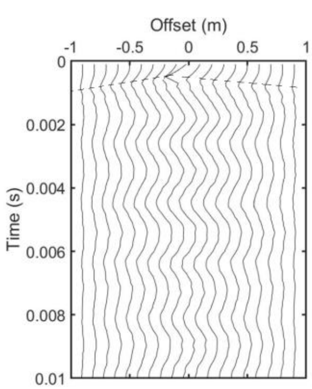

Figure 4: Synthetic shot gather data .

Conclusions

A non-linear implicit FEM code is developed in this work to solve the poro-visco-elasto-dynamics (Biot's) equations that represent the seismic behavior of fluid saturated porous media. The code can be instrumental in performing inverse modeling for hydro-carbon reservoir exploration. The workability of the code is demonstrated through a two-dimensional problem of a three-layered porous solid. From the simulations it is observed that the wave front propagates with the expected behavior in the top layer with abrupt transitions at the interfaces. This behavior is due to the modified intrinsic wave velocities in these three different layers. A shot gather response is also shown and it follows the expected trend.

Future work includes implementation of infinite boundaries so that experimentally consistent shot gather data can be generated. From the code perspective, sparse matrix solver needs to be incorporated to reduce the computational time significantly.

References

Belytschko, T., Liu, W. K., Moran, B., and Elkhodary, K., Nonlinear Finite Elements for Continua and Structures, 2nd Edition.

Biot, M. A., 1956a, Theory of propagation of elastic waves in a fluid-saturated porous solid. I: Low-frequency range: Journal of the Acoustical Society of America, 28, 168–178.

Biot, M. A., 1956b, Theory of propagation of elastic waves in a fluid-saturated porous solid. II: Higher-frequency range: Journal of the Acoustical Society of America, 28, 179–191.

Carcione, J. M., Herman, G. C. and Kroode, A. P. E., 2002, Seismic modeling, Geophysics, 67(4), 1304–1325.

Hickey, C. J., and J. M. Sabatier, 1997, Choosing Biot parameters for modeling water-saturated sand: Journal of the Acoustical Society of America, 102, 1480–1484.

Martin, R., Komatitsch, D., and Ezziani, A., An unsplit convolutional perfectly matched layer improved at grazing incidence for seismic wave propagation in poroelastic media, 2008, Geophysics, 73, 51-61.

Quiroga-Goode, G., Jimenez-Hernandez, S., Perez-Flores, M. A., and Padilla-Hernandez, R., 2005, Computational study of seismic waves in homogeneous dynamic-porosity media with thermal and fluid relaxation: Gauging Biot theory: Journal of Geophysical Research, 110, B07303.

FEM based Seismic Modeling

Acknowledgements:

We are thankful to Oil and Natural Gas corporation limited for the financial support.